

Full-Scale SHM of a Prestressed Concrete Bridge in Germany: Overview and Lessons Learned from a Long-Term Monitoring Campaign

Felipe Isamu Harger Sakiyama¹, Gustavo de Souza Veríssimo², Frank A. Lehmann³

¹ Universidade Federal dos Vales do Jequitinhonha e Mucuri, Instituto de Ciência, Engenharia e Tecnologia, felipe.sakiyama@ufvjm.edu.br

² Universidade Federal de Viçosa, Departamento de Engenharia Civil, gustavo@ufv.br

³ Materialprüfungsanstalt Universität Stuttgart, Germany, frank.lehmann@mpa.uni-stuttgart.de

Abstract

The ability to track the structural condition of existing structures is one of the main concerns of bridge owners and operators. The increasing demand for civil infrastructures, the aging of existing assets, and the strengthening of safety and liability laws have led to the inclusion of structural health monitoring (SHM) techniques in the structural management process. Furthermore, with the latest developments in the sensors field and computational power, real-scale SHM systems' deployment has become logistically and economically feasible. From this perspective, extensive research on structural health monitoring has been developed in the last decades. However, the transfer rate from laboratory experiments to real-case applications is still unsatisfactory. This paper addresses the deployment of a real-case SHM system based on long-gauge FBG sensors (LGFBG) on a 60-year-old prestressed highway bridge in Neckarsulm, Germany. The system has been running uninterruptedly for over three years, generating dozens of terabytes of measured data. The authors present an overview of the deployed SHM system, including: the data management system developed to handle large amounts of data; the novel real-time analysis algorithm for condition monitoring designed to automatically detect unexpected events within a multitude of random dynamic loads; and the hybrid methodology for model updating and damage identification built on data feature extraction using the principal component analysis (PCA), finite element (FE) simulation, and stochastic simulation to quantify the damage level of the monitored prestressed bridge. Finally, the authors discuss the main contributions to the field of SHM as well as the lessons learned during the three years of the monitoring campaign.

Keywords

Structural Health Monitoring, FBG sensors, long-term monitoring, model updating.

Introduction

Transportation infrastructure plays a crucial role in our society, enabling people to engage in activities that produce private, public, and social benefits (Frischmann 2012). With relevance to large structures, bridge structures are built to connect people, shorten travel time, cross obstacles, improve traffic flow at complex crossroads, and allow access to inaccessible regions. In this sense, the socioeconomic impact of an inoperant bridge and the life-threatening consequences of a damaged and unattended bridge network can be immeasurable. Hence, the capability to detect, quantify, and predict damages is the utmost desire of bridge owners to allow an effective and safe structural condition

assessment. Traditionally, the practice of periodic visual inspection predominates in maintenance programs throughout the world (Li et al. 2016). However, it is known that visual inspections are insufficient to satisfy the current needs for bridge maintenance (Cho et al. 2015; Lynch 2007). Therefore, including non-destructive damage detection and structural health monitoring (SHM) techniques in the structural management process has become increasingly sought (Jang et al. 2011; Spencer et al. 2004).

SHM strategies can be divided into two categories according to the presence or absence of physics-based numerical models: model-based and data-driven methods (Catbas et al. 2013). Model-based methods, also known as behavior models, are typically run by optimizing the discrepancy between measured structural responses and FE model predictions in a process called model updating.

The data-driven methods, called model-free, dispense information about structural physical responses. Instead, statistical parameters sensitive to structural changes are extracted from a baseline condition using approaches such as the principal component analysis (PCA) (Kumar et al. 2020), robust regression analysis (RRA) (Kromanis and Kripakaran 2014), and multi-linear regression (MRL) (Cavadas et al. 2013). Therefore, in SHM of existing structures where the detection of new damages and the estimation of the actual structural deterioration level are desired, the advantages of data-driven and model-based methods can be combined to enhance the condition assessment process (Malekzadeh et al. 2015).

Although many successful deployments of SHM on large structures have been presented (Malekzadeh et al. 2015; Meixedo et al. 2021), there is still a need for investigating and developing damage identification and performance assessment of concrete bridges. For most damage identification approaches, the stochastic nature of the damage formation and traffic loading is not considered simultaneously. Therefore, they cannot cope with the random damage scenarios and loading cases of existing highway prestressed bridges, e.g., where tendon breaks can occur in any section, and localized stiffness reductions may be inherited back from the construction phase. Moreover, the structural response of statically indeterminate structures such as prestressed bridges is sensitive to stiffness changes. Consequently, a sensor's abnormal behavior may be caused by damages at its location or by a combination of damages scattered in the structure. Thus, it is paramount that the SHM system of real-size concrete structures is designed with appropriate sensor count, area coverage, and optimized placement to assess the damage distribution correctly. Likewise, a damage detection method should be able to evaluate the sensors' damage feature sensitivity to stochastic damage scenarios for a reliable damage assessment.

This paper presents a novel algorithm for the real-time analysis and alarm triggering of a high sensor-count monitoring system deployed on a structure subjected to environmental and random dynamic loading. The SHM system is based on a long-gauge FBG (LGFBG) sensor network and was installed on a real-life prestressed concrete national highway bridge in Neckarsulm, Germany. Moreover, the authors propose a hybrid methodology that combines data-driven and finite element model (FEM) updating approaches to quantify the actual damage level of discretized length segments in terms of stiffness reduction of the prestressed concrete bridge in Neckarsulm. First, the dynamic strain data are analyzed using PCA to extract statistical parameters describing the static structural response traffic-induced loads. Next, a FEM of the prestressed bridge was implemented to simulate the real sensors' PCA response during traffic loading. At last, a sensitivity study is set to evaluate the impact of multiple damage scenarios on the extracted PCA features. The model updating is then processed using a Monte Carlo simulation by optimizing the difference between the simulated and measured PCA results.

Finally, the authors discuss the main contributions to the field of SHM as well as the lessons learned during the three years of the monitoring campaign.

SHM system in Neckarsulm

Characteristics of the monitored bridge

The monitored structure is a prestressed hollow-core concrete bridge constructed in 1964. It has three continuous spans without coupling joints with a total length of 57.00 m (17.00 m–23.00 m–17.00 m) and a width of 11.08 m (Figure 1.a and Figure 1.b). Two linear rocker bearings support the superstructure on the southern abutment and the northern abutment by two roller bearings. Like most prestressed concrete structures designed until the '70s in Germany, the bridge was built with prestressing steel known for its high vulnerability to corrosion-induced cracking (Wüstholtz 2016).

In addition to the high increase in traffic loads compared to the year of construction in 1964 and the corrosion-induced cracking risk, other critical problems may arise due to construction methods and the design standards adopted. Construction failures can already appear during construction caused by misplacement of the hollow-core bodies and difficulties in compacting the surrounding concrete. From the structural point of view, the hollow-core bodies prevent two-axis load transfer. Likewise, shear forces and temperature loads were not considered to the extent that it is deemed necessary by today's standards when the building was planned. Finally, the hollow core cannot be examined during the building inspection, so any damage inside them may not be detected early.

A FEM was built using the SOFiSTiK Bridge Design module. The Bridge Design module has a parametric design tool that optimizes the construction of the structure's geometry and allows the easy modeling of complex forms, such as curvatures and inclinations, and the prestressing system and tendons' geometry. The goal was to build a FEM close to the bridge's original blueprints. The structure parts were defined as beam elements, with 197 beam elements for the main deck and 50 for the columns. Figure 1.c shows an overview of the FE model in SOFiSTiK.

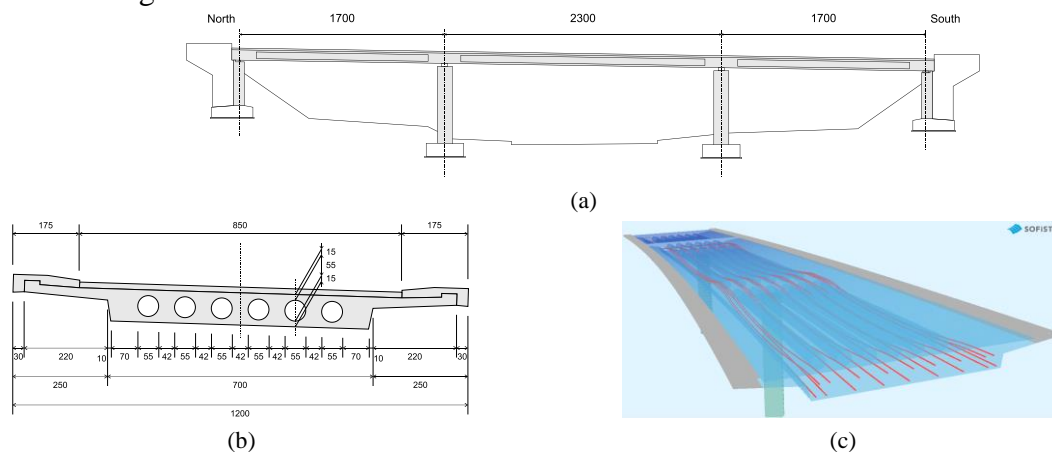


Figure 1. Monitored bridge: (a) Longitudinal view of the bridge (dimensions in meters); (b) Bridge's cross-section (dimensions in centimeters); (c) FE model in SOFiSTiK: main deck's cross-section and prestressing tendons.

Characteristics of the monitoring system

A fiber-optic (FO) monitoring system based on long-gauge FBG (LGFBG) sensors was installed to continuously monitor strain and temperature changes of the bridge superstructure. The strain monitoring in the longitudinal direction consists of two parallel measuring lines, each with 27 LGFBG sensors connected in a series along the complete longitudinal length, hereby defined as northbound sensors (S01 to S27) and southbound sensors (S28 to S54). For every LGFBG strain sensor, an embedded temperature sensor is present for temperature compensation on the FO. A schema of the sensors is given in Figure 2, and overview photos are shown in Figure 3. The LGFBG sensors have a gauge length of 2 meters. Additionally, 35 LGFBG sensors with a gauge length of 1.35 meters were installed, forming five lines of sensors in the transversal direction. However, they are not in the scope of this paper.

The monitoring system in Neckarsulm has run continuously since November 2019 at a sampling rate of 200 Hz, generating over 70 thousand measurement points per second. The sampling rate was defined to optimize the representation of extreme values, such as load peaks during a vehicle's crossing. Considering that the average travelling speed at the bridge is 60 km/h (and there are speed cameras a few meters from the north abutment), a sampling rate of 200 Hz provides an 8-centimeter measuring step. A comprehensive description of the monitoring system and the data management solution can be found in (Sakiyama et al. 2021a). More information about the LGFBG sensors and fiber optic sensing in SHM of concrete structures can be found in (Fackler July 2019; Lehmann et al. 2019; Sakiyama et al. 2021b; Sakiyama et al. 2022). More information on data handling and management can be found in (Sakiyama et al. 2021a). All the implemented scripts in MATLAB are available in (Sakiyama 2021a).

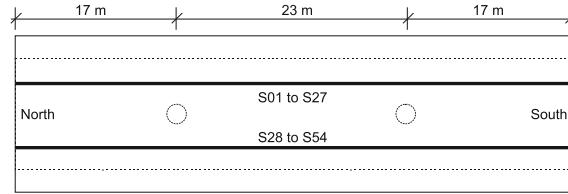


Figure 2. Schema of the sensors' configuration (bottom view of the superstructure).



Figure 3. Overview of the bridge and the monitoring system: (a) Sensor distribution; (b) An LGFBG sensor with a 2.05 m gauge.

Real-time analysis algorithm

An algorithm was developed and implemented for the installed SHM system in Neckarsulm to determine whether unexpected changes have occurred in the structure based on the real-time analysis of the measured strain and temperature data. The algorithm is registered for a patent. Statistical values are continuously updated from the strain and temperature data stream of each sensor over an optimized n -sampled moving time window τ_n , namely the statistical strain mode Mo , the arithmetic strain mean μ , the arithmetic temperature mean \bar{T} , and the maximal peak-to-peak amplitude u . Additionally, the strain data from the time window τ_n for every two adjacent sensors p and q are analyzed, where the correlation coefficient $\rho_{pq}(\tau_n)$ for the measured strain $s_p(k)$ and $s_q(k)$ are calculated according to the following:

$$\rho_{pq}(\tau_n) = \frac{\sum_{k=1}^n (s_{p,k} - \mu_p) \cdot (s_{q,k} - \mu_q)}{\sqrt{\sum_{k=1}^n (s_{p,k} - \mu_p)^2} \cdot \sqrt{\sum_{k=1}^n (s_{q,k} - \mu_q)^2}} \quad (1)$$

For a continuous monitoring system with high sampling rate measurements on coherent structures with consistent loading, the correlation coefficient between a pair of sensors must remain constant and close to one, if they are well correlated, or close to zero, if there is no correlation. In the case of adjacent sensors disposed along the longitudinal direction of a continuous beam, the correlation coefficient should remain stationary and close to one until a change occurs in the structural system (Catbas et al. 2012). The evaluation of the correlation between two sensors can also be used to infer already existing geometric discontinuities, e.g., hollow bodies or built-in parts, or pre-existing damages in the structure.

Although the correlation coefficient is a relevant parameter, it cannot be used alone as an indicator of structural change since noise and influences from wind or traffic loads, amongst others, can also lead to temporary deviations in the correlation. Therefore, the implemented algorithm is based on a three-step validation to avoid false calls and enhance the system's reliability. Should the correlation coefficient for two correlated sensors drop below a pre-defined threshold within the time window τ_n , the maximal peak-to-peak amplitude u and the strain-offset through the statistical mode Mo of both sensors during τ_n are examined. Under normal operation conditions, the peak-to-peak amplitude is directly related to the traffic load. Simultaneously, the statistical mode represents the stationary strain signal offset due to the environment temperature variation and can be considered the "unloaded state" of the bridge for a short time window. Therefore, suitable limit values must be defined for all three indicators. Since no load test was performed on the monitored bridge, the parameters' thresholds were taken from statistical analysis of a one-year measurement period. The correlation coefficient threshold was set as $\rho \leq 0.90$; the peak-to-peak amplitude limit was set up as $u \leq 60 \mu\text{m/m}$, and the statistical strain mode variation to $\Delta Mo \geq 25 \text{ mm/m}$.

In contrast to the traditional alarm-triggering approaches, the monitoring system in Neckarsulm does not rely on absolute or singular thresholds. Each derived parameter is particularly sensitive to different factors: the statistical strain mode to the temperature influence, the peak-to-peak strain amplitude to the traffic load, and the correlation coefficients to the static system behavior. If the three indicators individually show critical values, an alarm is triggered, allowing the bridge managers to evaluate all three indicators together with the complete sensor measurement data. The proposed system enables the detection of unexpected events by the minute and post-processing of the acquired data for long-term analysis of the structural integrity and life expectancy.

More details and results related to the real-time analysis algorithm can be found in (Sakiyama et al. 2021a).

A hybrid methodology for damage identification and quantification

The proposed hybrid methodology is divided into two main tasks: the data-driven tasks (SHM system) and the model-based tasks (FEM). The methodology's core is the strain feature extraction using the PCA method, which is performed for both the dynamic strain history from the SHM system and the FEM's simulated results. However, the tasks that precede the PCA analysis in each task have fundamental differences, especially during the data preparation. The SHM system, for example, runs uninterruptedly with a high sampling rate (200 Hz) and is subject to random load cases and environmental and operational variations. Therefore, a clustering algorithm was implemented to extract consistent data correlating with the simulated FEM results (Sakiyama 2021b). As for the FEM, the damage locations and their intensities are unknown. Hence, sensitivity analysis and a Monte Carlo simulation test millions of damage combinations and intensities cases. More details on the hybrid methodology implementation and results can be found in (Sakiyama et al. 2023).

PCA analysis of the SHM measurements

The principal component analysis (PCA) is a quantitative method to simplify multivariate statistics problems by replacing the original data with a new set of variables containing most of the information, called the principal components (MATLAB 2020). The principal components have no physical meaning, but they describe the directions explaining a maximum amount of variance, i.e., the axes that provide the best angle to see and evaluate the data. Those axes are called eigenvectors. There are as many eigenvectors as there are variables, with each eigenvector having the number of elements equal to the number of variables (e.g., the number of sensors) and an eigenvalue associated with it. Suppose the eigenvectors are sorted by their eigenvalues in decreasing order. In that case, they are arranged in order of significance, resulting in an $N \times N$ matrix, also called the principal components (PC) matrix, where N is the number of variables. The first principal component

comprises the axes' directions (i.e., the eigenvector) that capture each variable's largest possible variance. The second principal component is another set of axes perpendicular to the first and accounts for the following highest variance. This process continues until the number of calculated principal components equals the number of variables in the original data. However, it is a commonplace that the first few principal components explain over 80% of the total variance. Therefore, they can be used to understand the driving forces that generated the original data (Jaadi 2019).

The eigenvectors' elements can be understood as a "score" given to each sensor. The larger the score, the greater the influence of that sensor on the system's variance and driving forces. Thus, in a stable system, the sensors' scores should remain constant for load cases of the same nature. In other words, it is expected that the response of a given section in the structure, and thus the sensor installed on it, will be the same every time a vehicle crosses the bridge. Likewise, if that same structural section alters, e.g., due to stiffness degradation, the section's score will change, thus, the eigenvector element associated with it. Therefore, the PCA can constantly evaluate changes in the system's behavior from the structure's measured history and allow damage identification with the structure under regular operation.

To assure damage identification reliability, an important task is to characterize the load cases that will be assessed. For a bridge structure, it is reasonable to consider the crossing of a single heavy vehicle as the most representative external load. However, vehicles with different velocities, weights, lengths, and axle numbers cross the bridge at a random pace. Moreover, multiple heavy vehicles may cross the bridge simultaneously and in opposite directions. Therefore, a clustering algorithm was developed to identify when a single vehicle crosses the bridge and categorize the recorded vehicles' crossing about their number of axles, total length, and travel direction. Representative load cases were then filtered and defined from the classified traffic information having the following constraints:

- The crossing of a single heavy vehicle (in either direction);
- Number of identified axles equal to or higher than two;
- Average velocity smaller than 30 m/s (108 km/h);
- Maximal strain at the bridge's midpoint higher than 20 $\mu\text{m/m}$.

From the over 60 thousand recorded crossings, 11,470 were within those constraints. The vehicles' length was found to be the parameter that impacts the strain histories' response most when considering vehicles within the road's allowed weight.

With the classified vehicle data, the PCA analysis calculates each sensor's contribution to the structural response. Figure 4, e.g., shows the average PCA results for 1,476 crossings in the northbound direction (S01 to S27) of a vehicle category defined as group 7 (vehicles with a total length from 9 to 10 meters). Only the first four eigenvectors with higher eigenvalues, i.e., the first four principal components (PC), are analyzed as they explain over 95% of the system's variance. Figure 4.a depicts the first and second principal components' eigenvectors, and Figure 4.b the eigenvectors for the third and fourth principal components. The individual eigenvectors' elements corresponding to each sensor are depicted with either circles or x-markers and connected with lines for visualization. In Figure 4.c, the respective first principal component's eigenvector for sensors S07 and S14 are shown for one year and four months. Their average values are depicted with dashed horizontal lines. Continuously horizontal lines define the range plus-minus two times their standard deviation for the period. Figure 4.d shows how much the first four principal components explain the system's variance. From the first to the fourth PC, the variance explained were: 59.4%, 23.9%, 7.3%, and 4.6%.

FE model sensitivity analysis

Defining the PC eigenvectors' sensitivity to structural changes in the FE model is necessary to use the PCA analysis in the model updating process. Moreover, the FE model's PCA results must be compatible and comparable to the PCA results from the SHM measurements. Therefore, the following workflow is proposed:

- Define a load train model consistent with a vehicle length category to simulate a vehicle's crossing;
- Establish a FEM that mimics the results from the real SHM system;
- Apply the load train on the undamaged FEM and run the PCA analysis for its results;
- Introduce damage in various known cross-sections;
- For each damage case, apply the load train on the damaged model and run the PCA analysis for the FEM results;
- Analyze the PC eigenvectors (from the first four PC) changes between the damage cases and the undamaged structure.

The damage cases were defined in the FEM by reducing the bending stiffness of the elements corresponding to each of the 27 sensors' positions at a time. Then, the load train was applied for each damage case, and the PCA analysis of the FEM results was calculated. Therefore, it is possible to assess how the principal components' eigenvectors and their elements change for each damage case and which damage cases impact the overall structural response more.

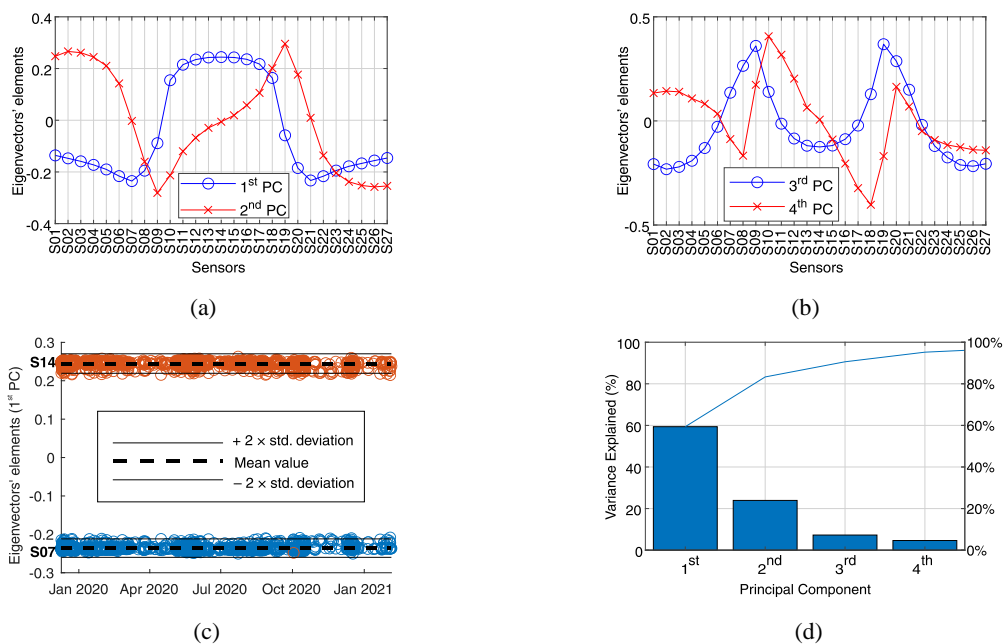


Figure 4. Average results of the PCA analysis for group 7 in the northbound direction (S01 to S27). The lines connecting the eigenvectors' elements are only to improve visualization and have no physical meaning: (a) Eigenvectors for the first and second principal components (PC); (b) Eigenvectors for the second and third PC; (c) Eigenvectors' elements for the first principal component over time – sensors S07 and S14; (d) Variance explained by the first four PC.

FE model updating

The proposed model updating process is based on the range-normalized root mean square error (NRMSE) optimization between the PCA results from the real SHM system and the FEM. As mentioned, the results are similar for the northbound (sensors S01 to S27) and southbound (sensors S28 to S54). Therefore, only the results for the northbound traffic (sensors S01 to S27) are presented for representation.

First, the PCA results from group category 7 with northbound travel direction are selected as the real reference case, and the trainload LM4 type 3 as the reference load case for the FEM results. The process starts with the NRMSE for the undamaged FEM, which will be referenced from now on as the undamaged model. Next, a Monte Carlo objective function based on the FE sensitivity analysis optimizes the NRMSE by applying a combination of stiffness reduction factors (FACS) to select an initial damaged model. Finally, the initial damaged model undergoes refinements in an iterative optimization procedure until the NRMSE result converges.

Figure 5 shows the entire model updating process, where the eigenvectors' average NRMSE for each iteration is depicted with blue circles. The first iteration corresponds to the undamaged model with an average NRMSE of 4.17%. After running the first iteration, the eigenvectors' average NRMSE drops to 2.56%, which defines the initial damaged model. Next, the refinement process is repeated until the 18th iteration, when the final damaged model with an average NRMSE of 2.48% is reached. The iterations' average NRMSE gradient is plotted on the right y-axis and represented with a continuous orange line. The gradient oscillates until the 14th iteration, starting to converge to zero up to the 18th iteration. The Monte Carlo approach allows the indirect evaluation of millions of damage combinations and intensities during the model updating process using a quasi-random Sobol sequence, which would be unfeasible if a FE simulation had to be executed for each damage scenario. For example, for the model updating presented in Figure 5, 144 million damage scenarios could be tested, while only 18 FE simulations were necessary.

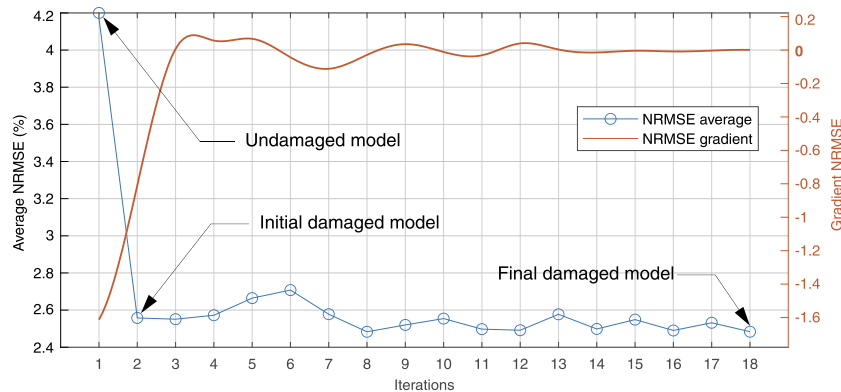


Figure 5. Average NRMSE during the model updating iterations. Iteration 1 represents the undamaged model, iteration 2 is the initial damaged model, and iteration 18 is the final damaged model. The convergence is shown as the NRMSE gradient.

Table 1 shows the eigenvectors' average NRMSE value for the undamaged, initial, and final damaged models. The final NRMSE reduction between the final damaged and undamaged models is shown in the last column. The best improvement was in the third PC eigenvector, with an NRMSE decrease of 67.75%, followed by the first and fourth PC, showing reductions of 31.12% and 30.70%, and ending with the second PC, which was increased by 3.14%. The eigenvectors' average NRMSE was reduced by 42.33%.

Table 1. NRMSE values during the model updating process for the undamaged, initial, and final damaged models. The last column shows the NRMSE reduction between the final damaged and undamaged models.

Iteration \ PC	Eigenvectors' NRMSE (%)			NRMSE final reduction (%)
	1 st – Undamaged model	2 nd – Initial damaged model	18 th – Final damaged model	
1 st PC	1.96	1.42	1.35	-31.12
2 nd PC	2.23	2.46	2.30	+3.14
3 rd PC	7.30	2.38	2.34	-67.75
4 th PC	5.70	3.97	3.95	-30.70
Average	4.30	2.56	2.48	-42.33

The stiffness reduction factors (FACS) in the final damaged FE model are depicted as a heatmap in Figure 6. The values correspond to the total stiffness reduction applied in the beam elements at each sensor location. A maximum stiffness reduction is observed at sensors S16 and S09, with a decrease of 15.5% and 13.5%, respectively. The beam elements in the first spam (S01-S07) have a minor stiffness reduction, with reduction values inferior to 2%. Next, the last spam beam elements (S21-S27) have stiffness reduction values ranging from zero to 9.3%. Finally, the mid-spam has the most significant reduction factors, ranging from zero to 15.15%. The facticity of the calibration results was verified by comparing the sections' stiffness reductions with in-field visual data. The first spam comprised of sensors S01 to S06 is the bridge's region with the least visible damage, which coincides with the small stiffness reduction factors.

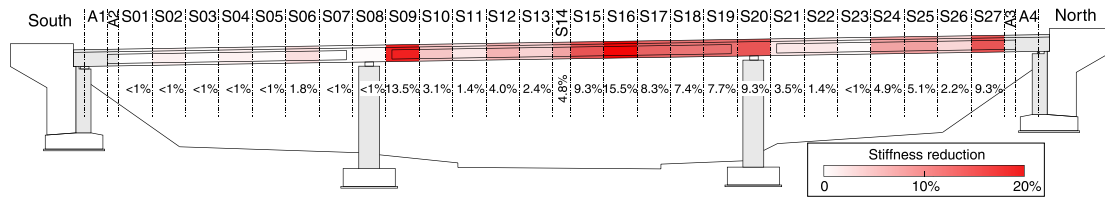


Figure 6. Stiffness reduction factors (FACS) applied in the beam elements of the final damaged FE model.

Conclusion

In this work, the authors presented an overview of the deployed SHM system on a prestressed concrete bridge in Neckarsulm, Germany, in operation since 2019. In addition, the proposed novel real-time analysis algorithm for detecting unexpected events and the hybrid methodology for damage identification was presented. From the results and experience acquired during the monitoring campaign, the following conclusions are drawn:

- A robust and autonomous data management system is fundamental to handling a high sensor-count monitoring system in real-case SHM applications. It must be able to pre-process the raw data and store it on a reliable database to allow efficient data selection for post-processing to evaluate long-term structural changes.

- The sensor type, area coverage, and sensor count are essential to analyze while developing and deploying a real-size SHM system. In addition, for concrete structures with statically indeterminate behavior, a representative area of the structure must be measured to correctly depict its behavior and allow the detection of local damages, such as cracks and ruptures in prestressed tendons.

- The proposed real-time analysis algorithm addressed many known limitations of real-case SHM systems. The algorithm runs autonomously in runtime inside the acquisition software and can detect unexpected changes with a low false call rate by the minute. Moreover, the algorithm resolution to identify the unexpected changes' location is as small as the sensor's gauge lengths. Finally, the three-step alarm triggering responds to random and dynamic loads. It is free from environmental influences and is not tied to pre-defined failure modes or absolute limit values.

- In statically indeterminate structures, local changes may result from multiple damage cases rather than damage located only at the sensor presenting abnormal behavior. Therefore, individual sensor response changes should not be interpreted as damage limited to that sensor's locations. The sensitivity analysis in the FEM showed that damage at a sensor's location could impact the PCA results at multiple locations. In this sense, the model updating process should not treat each sensor's response individually but take complete account of the sensor's sensitivity to the structure changes.

- Considering the stochastic nature of damage events, it is unfeasible to simulate the necessary damage scenarios to optimize the FEM objective function accurately. Therefore, a Monte Carlo simulation was implemented using a quasi-random Sobol sequence with millions of combinations for damage location and intensity. The Monte Carlo simulation is repeated for each FEM simulation step, allowing the objective function to converge with only 18 FEM simulation iterations.

- The PCA analysis can extract the driving principles of the structure's static response during individual vehicles' crossings and eliminate external influences such as environmental and operation variations. In addition, the damage identification reliability was improved by considering not only the eigenvector representing the first PC, but all eigenvectors explaining up to 95% of the static response's variance.

The reliable assessment of the structure's damage state can lead to a rational structural conditional assessment. In addition, the optimized FEM can be used to check if the structure meets safety and serviceability requirements continuously. Likewise, visual inspection and in situ non-destructive tests could be prioritized where damage is most likely present. Finally, the structure's remaining lifetime can be locally evaluated, allowing the optimization of interventions and repairs.

Acknowledgement

The authors are grateful for the financial support from the Universidade Federal dos Vales do Jequitinhonha e Mucuri (UFVJM).

References

- Catbas, F. N., H. B. Gokce, and M. Gul. 2012. "Nonparametric analysis of structural health monitoring data for identification and localization of changes: Concept, lab, and real-life studies." *Structural Health Monitoring* 11 (5), 613–626. <https://doi.org/10.1177/1475921712451955>.
- Catbas, F. N., T. L. Kijewski-Correa, and A. E. Aktan. 2013. *Structural identification of constructed systems: Approaches, methods, and technologies for effective practice of St-Id*. Reston Virginia: American Society of Civil Engineers.
- Cavadas, F., I. F. Smith, and J. Figueiras. 2013. "Damage detection using data-driven methods applied to moving-load responses." *Mechanical Systems and Signal Processing* 39 (1-2), 409–425. <https://doi.org/10.1016/j.ymssp.2013.02.019>.
- Cho, S., R. K. Giles, and B. F. Spencer. 2015. "System identification of a historic swing truss bridge using a wireless sensor network employing orientation correction." *Struct. Control Health Monit.* 22 (2), 255–272. <https://doi.org/10.1002/stc.1672>.
- Fackler, R. M. 2019. *Einsatz von faseroptischen Messsystemen mit FBGs an einer Spannbetonbrücke auf Basis von Laborversuchen*, Master's thesis.
- Frischmann, B. M. 2012. *Infrastructure: The social value of shared resources / Brett M. Frischmann*. New York: Oxford University Press.
- Jaadi, Z. 2019. "A Step-by-Step Explanation of Principal Component Analysis." <https://builtin.com/data-science/step-step-explanation-principal-component-analysis>.
- Jang, S., S.-H. Sim, H. Jo, and J. F. Spencer. 2011. "Full-scale decentralized damage identification using wireless smart sensors." In *Proc., SPIE Smart Structures and Materials + Non-destructive Evaluation and Health Monitoring*, edited by M. Tomizuka, SPIE Proceedings, 79814W. <https://doi.org/10.1117/12.881160>.
- Kromanis, R., and P. Kripakaran. 2014. "Predicting thermal response of bridges using regression models derived from measurement histories." *Computers & Structures* 136, 64–77. <https://doi.org/10.1016/j.compstruc.2014.01.026>.
- Kumar, K., P. K. Biswas, and N. Dhang. 2020. "Time series-based SHM using PCA with application to ASCE benchmark structure." *J Civil Struct Health Monit* 10 (5), 899–911. <https://doi.org/10.1007/s13349-020-00423-2>.
- Lehmann, F. A., F. I. H. Sakiyama, and R. M. Fackler. 2019. "Fibre optic measurement systems for building monitoring." *Otto-Graf-Journal* 18, 183–196.
- Li, J., K. A. Mechtov, R. E. Kim, and B. F. Spencer. 2016. "Efficient time synchronization for structural health monitoring using wireless smart sensor networks." *Struct. Control Health Monit.* 23 (3), 470–486. <https://doi.org/10.1002/stc.1782>.
- Lynch, J. P. 2007. "An overview of wireless structural health monitoring for civil structures." *Philosophical Transactions of The Royal Society*, 345–372. <https://doi.org/10.1098/rsta>.
- Malekzadeh, M., G. Atia, and F. N. Catbas. 2015. "Performance-based structural health monitoring through an innovative hybrid data interpretation framework." *J Civil Struct Health Monit* 5 (3), 287–305. <https://doi.org/10.1007/s13349-015-0118-7>.
- MATLAB. 2020, version 9.9.0 (R2020b). Natick, Massachusetts: The MathWorks, Inc.
- Meixedo, A. et al. 2021. "Damage detection in railway bridges using traffic-induced dynamic responses." *Engineering Structures* 238, 112189. <https://doi.org/10.1016/j.engstruct.2021.112189>.
- Sakiyama, F. I. H. 2021a. *Implemented scripts for the operation and data analysis of a real-size SHM based on long-gauge FBG sensors*.
- Sakiyama, F. I. H. 2021b. *Real-size structural health monitoring of a prestressed concrete bridge based on long-gauge fiber Bragg grating sensors*. <https://doi.org/10.18419/opus-11681>.
- Sakiyama, F. I. H., F. Lehmann, and H. Garrecht. 2021a. "A Novel Runtime Algorithm for the Real-Time Analysis and Detection of Unexpected Changes in a Real-Size SHM Network with a Quasi-Distributed FBG Sensors." *Sensors* 21 (8), 2871. <https://doi.org/10.3390/s21082871>.
- Sakiyama, F. I. H., F. Lehmann, and H. Garrecht. 2021b. "Structural health monitoring of concrete structures using fibre-optic-based sensors: a review." *Magazine of Concrete Research* 73 (4), 174–194. <https://doi.org/10.1680/jmacr.19.00185>.
- Sakiyama, F. I. H., F. Lehmann, and H. Garrecht. 2022. "Deployment of a High Sensor-Count SHM of a Prestressed Concrete Bridge Using Fibre Optic Sensors." *3rd RILEM Spring Convention 2020 - Rilem Bookseries* 34, 183–195. https://doi.org/10.1007/978-3-030-76465-4_17.
- Sakiyama, F. I. H., G. S. Veríssimo, F. Lehmann, and H. Garrecht. 2023. "Quantifying the extent of local damage of a 60-year-old prestressed concrete bridge: A hybrid SHM approach." *Structural Health Monitoring* 22 (1), 496–517. <https://doi.org/10.1177/14759217221079295>.
- Spencer, B. F., M. E. Ruiz-Sandoval, and N. Kurata. 2004. "Smart sensing technology: opportunities and challenges." *Struct. Control Health Monit.* 11 (4), 349–368. <https://doi.org/10.1002/stc.48>.
- Wüstholtz, T. 2016. "Instandsetzung oder Neubau von Massivbrücken?: Erfahrungen und davon abgeleitete Ansätze.", edited by (Hg.) Bundesanstalt für Wasserbau, 23–41, Karlsruhe, Germany.